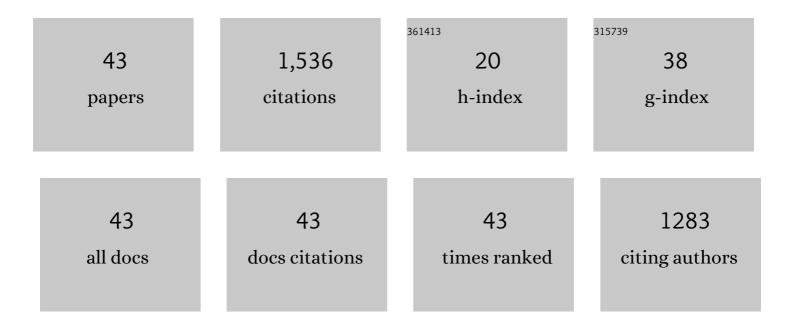
Fangqin Cheng

List of Publications by Year in descending order

Source: https://exaly.com/author-pdf/3813544/publications.pdf Version: 2024-02-01



#	Article	IF	CITATIONS
1	Employing an ICT-FRET Integration Platform for the Real-Time Tracking of SO ₂ Metabolism in Cancer Cells and Tumor Models. Journal of the American Chemical Society, 2020, 142, 6324-6331.	13.7	186
2	Heat Stroke in Cell Tissues Related to Sulfur Dioxide Level Is Precisely Monitored by Light-Controlled Fluorescent Probes. Journal of the American Chemical Society, 2020, 142, 3262-3268.	13.7	164
3	Ionic Liquid Droplet Microreactor for Catalysis Reactions Not at Equilibrium. Journal of the American Chemical Society, 2017, 139, 17387-17396.	13.7	130
4	A New Strategy: Distinguishable Multi-substance Detection, Multiple Pathway Tracing Based on a New Site Constructed by the Reaction Process and Its Tumor Targeting. Journal of the American Chemical Society, 2020, 142, 18706-18714.	13.7	114
5	Improved extraction of alumina from coal gangue by surface mechanically grinding modification. Powder Technology, 2016, 302, 33-41.	4.2	91
6	Novel process of alumina extraction from coal fly ash by pre-desilicating—Na2CO3 activation—Acid leaching technique. Hydrometallurgy, 2017, 169, 418-425.	4.3	88
7	Novel extraction of valuable metals from circulating fluidized bed-derived high-alumina fly ash by acid–alkali–based alternate method. Journal of Cleaner Production, 2019, 230, 302-313.	9.3	62
8	Liquid marble-derived solid-liquid hybrid superparticles for CO2 capture. Nature Communications, 2019, 10, 1854.	12.8	52
9	Dissolution kinetics of aluminum and iron from coal mining waste by hydrochloric acid. Chinese Journal of Chemical Engineering, 2015, 23, 590-596.	3.5	49
10	Interactions of coal gangue and pine sawdust during combustion of their blends studied using differential thermogravimetric analysis. Bioresource Technology, 2016, 214, 396-403.	9.6	48
11	Behaviors and Mechanism of Iron Extraction from Chloride Solutions Using Undiluted Cyphos IL 101. Industrial & Engineering Chemistry Research, 2015, 54, 7534-7542.	3.7	46
12	A simple hydrothermal synthesis of zeolite X from bauxite tailings for highly efficient adsorbing CO2 at room temperature. Microporous and Mesoporous Materials, 2019, 287, 77-84.	4.4	44
13	AlCl3â‹6H2O recovery from the acid leaching liquor of coal gangue by using concentrated hydrochloric inpouring. Separation and Purification Technology, 2015, 151, 177-183.	7.9	43
14	Low-Temperature Highly Efficient and Selective Removal of H ₂ S over Three-Dimensional Zn–Cu-Based Materials in an Anaerobic Environment. Environmental Science & Technology, 2020, 54, 5964-5972.	10.0	42
15	Heavy metal fixing and heat resistance abilities of coal fly ash-waste glass based geopolymers by hydrothermal hot pressing. Advanced Powder Technology, 2018, 29, 1487-1492.	4.1	34
16	Effect of oxygen concentration on oxy-fuel combustion characteristic and interactions of coal gangue and pine sawdust. Waste Management, 2019, 87, 288-294.	7.4	30
17	Distribution Characteristics of Valuable Elements, Al, Li, and Ga, and Rare Earth Elements in Feed Coal, Fly Ash, and Bottom Ash from a 300 MW Circulating Fluidized Bed Boiler. ACS Omega, 2019, 4, 6854-6863.	3.5	28
18	Pseudocapacitive Charge Storage in MXene–V ₂ O ₅ for Asymmetric Flexible Energy Storage Devices. ACS Applied Materials & Interfaces, 2020, 12, 54791-54797.	8.0	28

Fangqin Cheng

#	Article	IF	CITATIONS
19	Comprehensive evaluation of inherent mineral composition and carbon structure parameters on CO2 reactivity of metallurgical coke. Fuel, 2019, 235, 647-657.	6.4	26
20	Extraction of Valuable Metals and Preparation of Mesoporous Materials from Circulating Fluidized Bed-Derived Fly Ash via an Acid–Alkali-Based Alternate Method. ACS Omega, 2020, 5, 31295-31305.	3.5	24
21	Zeolite X Adsorbent with High Stability Synthesized from Bauxite Tailings for Cyclic Adsorption of CO ₂ . Energy & Fuels, 2019, 33, 6641-6649.	5.1	21
22	Recirculating coking by-products and waste for cost-effective activated carbon (AC) production and its application for treatment of SO2 and wastewater in coke-making plant. Journal of Cleaner Production, 2021, 280, 124375.	9.3	19
23	Indispensable role of inherent calcite in coal on activated carbon (AC)'s preparation and applications. Fuel, 2021, 287, 119481.	6.4	18
24	Experimental study on foam glass prepared by hydrothermal hot pressing-calcination technique using waste glass and fly ash. Ceramics International, 2021, 47, 28603-28613.	4.8	17
25	Synthesis and characterization of geopolymer prepared from circulating fluidized bed-derived fly ash. Ceramics International, 2022, 48, 11820-11829.	4.8	16
26	Coke powder improving the performance of desulfurized activated carbon from the cyclic thermal regeneration. Chemical Engineering Journal, 2022, 448, 137459.	12.7	16
27	One-Step Synthesis of Solid–Liquid Composite Microsphere for CO ₂ Capture. ACS Applied Materials & Interfaces, 2021, 13, 5814-5822.	8.0	14
28	Enhanced SO ₂ and Rhodamine B Removal by Blending Coke-Making Waste Benzene Residue (BR) for Pelletized Activated Coke (PAC) Production and Mechanisms. Energy & Fuels, 2019, 33, 5173-5181.	5.1	13
29	In-Suit Industrial Tests of the Highly Efficient Recovery of Waste Heat and Reutilization of the Hot Steel Slag. ACS Sustainable Chemistry and Engineering, 2021, 9, 3955-3962.	6.7	11
30	Effect of organic matter on the Rietveld quantitative analysis of crystalline minerals in coal gangue. Powder Diffraction, 2016, 31, 185-191.	0.2	10
31	Experimental investigation and cost assessment of the salt production by solar assisted evaporation of saturated brine. Chinese Journal of Chemical Engineering, 2018, 26, 701-707.	3.5	9
32	Hydrothermal synthesis of zeolitic material from circulating fluidized bed combustion fly ash for the highly efficient removal of lead from aqueous solution. Chinese Journal of Chemical Engineering, 2022, 47, 193-205.	3.5	9
33	Surface-Segregation-Induced Nanopapillae on FDTS-Blended PDMS Film and Implications in Wettability, Adhesion, and Friction Behaviors. ACS Applied Materials & Interfaces, 2018, 10, 7476-7486.	8.0	6
34	Insights into Coproduction of Silica Gel via Desulfurization of Steel Slag and Silica Gel Adsorption Performance. ACS Omega, 2022, 7, 21062-21074.	3.5	5
35	Phase Diagram of AlCl3–FeCl3–H2O(â~'HCl) Salt Water System at 298.15 K and Its Application in the Crystallization of AlCl3·6H2O. Journal of Chemical & Engineering Data, 2019, 64, 5089-5094.	1.9	4
36	Hydrothermal Hot-pressing Solidification of Coal Fly Ash and Its Ability of Fixing Heavy Metal. Journal of Residuals Science and Technology, 2015, 12, 143-148.	0.6	4

FANGQIN CHENG

#	Article	IF	CITATIONS
37	Separating NaCl and AlCl3·6H2O Crystals from Acidic Solution Assisted by the Non-Equilibrium Phase Diagram of AlCl3-NaCl-H2O(-HCl) Salt-Water System at 353.15 K. Crystals, 2017, 7, 244.	2.2	3
38	Dynamic Desulfurization Process over Porous Zn–Cu-Based Materials in a Packed Column: Adsorption Kinetics and Breakthrough Modeling. Energy & Fuels, 2020, 34, 16552-16559.	5.1	3
39	Fabrication of Mechanically Robust and Highly Elastic Epoxy Sponges <i>via</i> Surface Embedding of Nanoparticles for Long-Term Oil/Water Separation. ACS ES&T Engineering, 2022, 2, 924-939.	7.6	3
40	Al ₂ O ₃ Dispersion-Induced Micropapillae in an Epoxy Composite Coating and Implications in Thermal Conductivity. ACS Omega, 2021, 6, 17870-17879.	3.5	2
41	High-Strength Solidification of Fly Ash/Carbide Slag and Its Fixing Ability for Heavy Metals. Journal of Residuals Science and Technology, 2017, 14, 155-160.	0.6	2
42	Spinel Ferrite Transformation for an Efficient Fe Removal from Circulating Fluidized Bed Fly Ash by Carbothermal Reduction at a Low Temperature. ACS Omega, 2022, 7, 18612-18622.	3.5	2
43	Novel insight into composite packing of copper modified adsorbents for synergistically capturing H2S&HCl in low-temperature anaerobic environment. Separation and Purification Technology, 2021, 275, 119222.	7.9	Ο